Supplementary Information

3-Dimensional Graphene Decorated Copper-Phosphide (Cu_3P@3DG) Heterostructure as Effective Electrode for Supercapacitor

Subodh Kumar[1#], SK Tarik Aziz[1#], Sushil Kumar[2#], Sk Riyajuddin[2], Gili Yaniv[3], Louisa Meshi[3], Gilbert D. Nessim[1]* and Kaushik Ghosh[2]**

[1] *Department of Chemistry, Bar-Ilan Institute for Nanotechnology and Advanced Materials (BINA), Bar-Ilan University, Ramat Gan-52900, Israel. E-mail:* gdnessim@biu.ac.il

[2] *Institute of Nano Science & Technology, Habitat Centre, Phase-10, Sector-64, Mohali- 160062, India, E-mail:* kaushik@inst.ac.in

[3] *Department of Materials Engineering, Ben Gurion University of the Negev, Beer-Sheva 84105, POB 653, Israel. E-mail:* louisa@bgu.ac.il

Materials characterization

Scanning electron microscope (SEM) FEI Quanta FEG 250 and high-resolution SEM (HRSEM) FEI Magellan 400Li, comprising energy dispersive X-ray spectrometer (EDS), were used at 15kV to determine the surface morphology and elemental analysis. The specimens were also examined at 200 kV using a JEOL JEM-2100F Transmission Electron Microscope (TEM) equipped with a Thermo-Fisher Scientific EDS analyser and Gatan CCD camera. The TEM analysis was performed on powdered material dispersed on Au grids with amorphous carbon film. Phase content of synthesised materials was characterized by a powder X-ray diffraction pattern using a Bruker D8 Advance diffractometer at 40 kV and 40 mA with Cu Kα radiation (λ= 0.15418 nm) with a scan rate 10°/min. The FullProf program (J. Rodrigues-Carvajal, FullProf Suite, Version 2.05 (2011)) was used for the refinement of the structure. XPS analysis was performed in a Kratos AXIS-HS spectrometer, using a monochromatized Al Kα source. All XPS measurements were carried out at room temperature, under the vacuum of ~ 1×10^{-9} Torr. The porous surface area was measured by

BET (Quantachrome Instrument, version 3.01). Keithley Source meter 2450 was used for conductivity measurement.

Electrochemical measurements

The electrochemical properties of the as-synthesized product were carried out on a conventional three-electrode system (Metrohm Autolab electrochemical workstation) using 1.0 M Na_2SO_4 solution as the electrolyte at room temperature. The pure Cu_3P electrochemical performance was conducted on a precleaned glassy carbon electrode with the loading concentration of ~ 0.91 mg/cm^2 (65 µl was drop-casted from a stock solution of 5mg in 5 ml IPA) to cover the complete electrode surface (area 0.07 cm^2). The same loading concentration Cu_3P on graphite electrode was kept as ~ 0.91 mg/cm^2 where the 1ml stock solution was drop casted on 1x1 cm^2 graphite electrode. Simultaneously, the Cu_3P@3DG and 3DG electrodes had been designed on the graphite substrate and the electrochemical performance was tested in 1.0 M Na_2SO_4 medium. The cyclic voltammogram (CV), galvanostatic charge/discharge (GCD) and electrochemical impedance spectroscopy (EIS) measurements were performed using Cu_3P on glassy-carbon or Cu_3P@3DG or 3DG on graphite served as the working electrode, platinum wire as the counter electrode and Ag/AgCl (saturated 3.0 M KCl) as the reference electrode. The glassy carbon electrode was cleaned via a simple polishing technique with figure-eight motions on a cloth polishing pad in a water alumina slurry followed by water and ethanol bath sonication. The specific capacitance from the CV curves was calculated according to the following equation:

$C_{sp} = (\int IdV)/(\upsilon m \Delta V)$

According to the GCD results, the gravimetric specific capacitance (C_{sp}) can be calculated to the following equation:

$C_{sp} = I\Delta t/((\Delta V\text{-}IR)*m)$

Where C_{sp} is the specific capacitance (F/g), m is the corresponding mass loading of the active electrode material, ΔV is the voltage window, υ is the scan rate and I represent the current, Δt the period for a full discharge.

The energy density (E) was calculated from the specific capacitance (C_{sp}) and the cell potential (V) according to the following equation:

$$E\ (Wh/Kg) = 0.5 C_{sp} V^2 / 3.6$$

$$P\ (W/Kg) = E*3600/\Delta t$$

The coulombic efficiency of supercapacitors device was calculated by the following equation:

$$Q = C_{discharge}/C_{charge}$$

where Q is the coulombic efficiency, $C_{discharge}$ and C_{charge} are discharge specific capacitance and charge specific capacitance, respectively.

The EIS tests were performed at an open-circuit potential with AC amplitude at 5mV in a frequency range of 100 kHz - 0.1 Hz.

As shown in Fig. 2a, the average specific capacitance of hexagonal Cu_3P platelets was calculated to be 205, 165.28, 95.31, 82.63, and 68.38 F/g at the scan rate of 10, 50, 100, 150, and 200 mV/s, respectively. The increase in specific capacitance with the fall of the scan rate is due to the facile diffusion of electrolyte ions inside the inner layers of the active material, leading to higher interactions with the active sites of the electrode material for the charge transfer(Singh et al., 2017). There was no noticeable distortion of the CV curves when the scan rate varied from 10 to 200 mV/s, implying the fast charge-discharge performance of the Cu_3P electrode. Fig. 2b presents the typical galvanostatic charge-discharge voltage vs time profiles measurements of the Cu_3P platelets electrode at various current density, in potential window 1.0 V. The long charge and discharge

plateaus are noticed for all GCD curves which are consistent with the above-mentioned CV results. Impressively, the specific capacities of 254.8, 239.7, 234.8, 221.2 and 181.5 F/g at current densities of 0.8, 0.9, 1.28, 3.4 and 4.14 A/g are obtained, respectively.

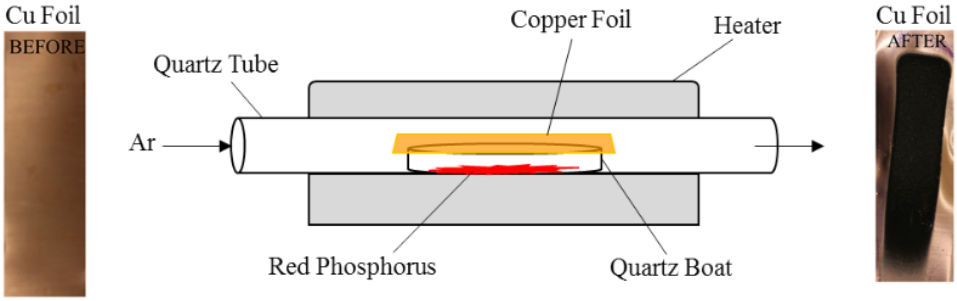

Fig. S1: Schematic diagram for the synthesis of Cu_3P on copper.

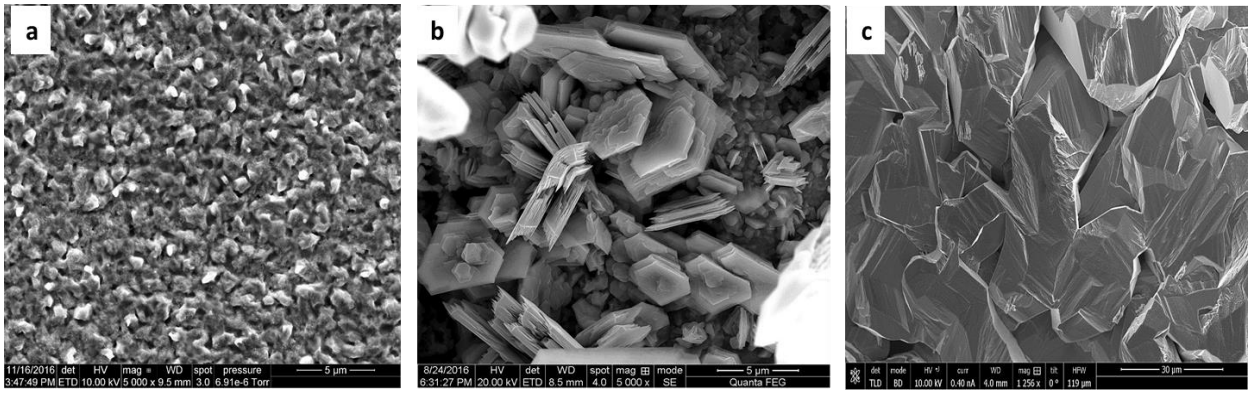

Fig. S2: Copper Phosphide growth at a) 350 °C, b) 600 °C, c) 800 °C temperature.

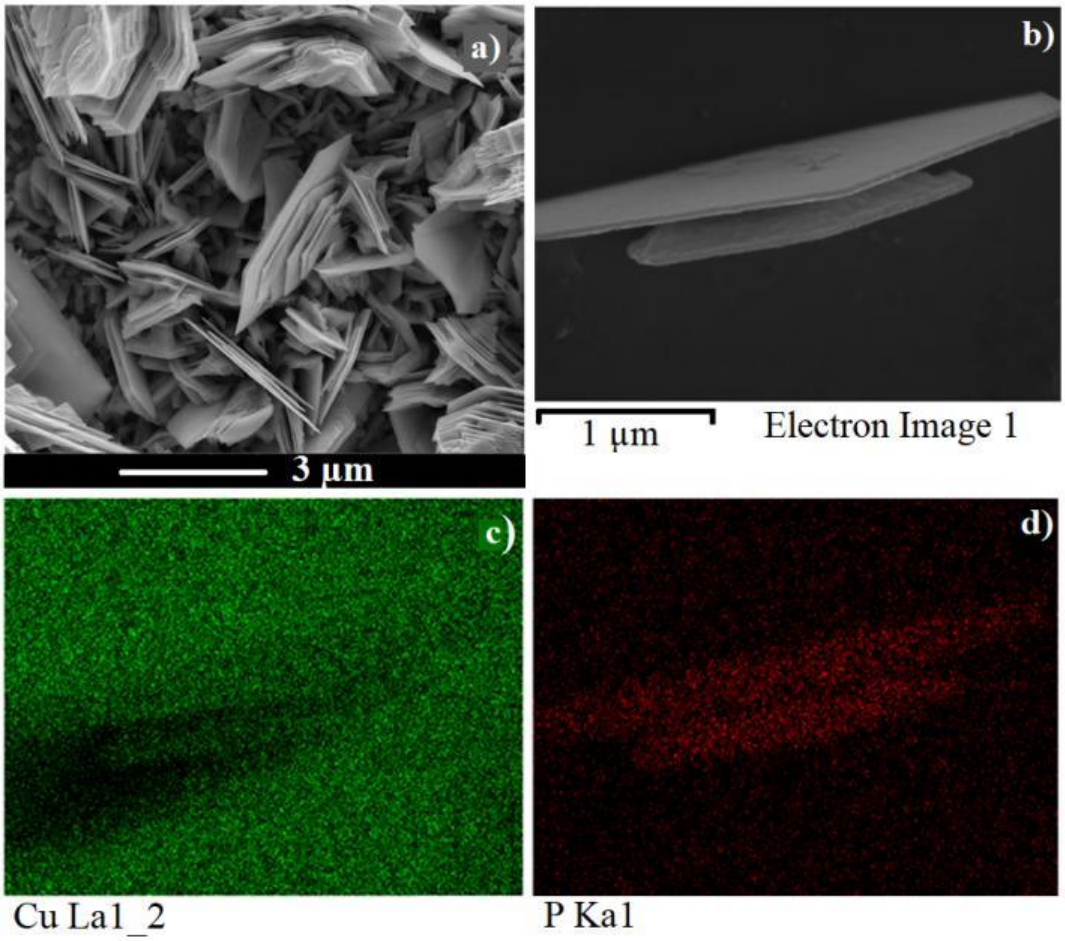

Fig. S3: a) HRSEM image of Cu_3P; b) hexagonal platelet for elemental mapping; (c-d) corresponding elemental mapping of Cu and P demonstrate that the Cu and P elements were uniformly distributed on the hexagonal platelets.

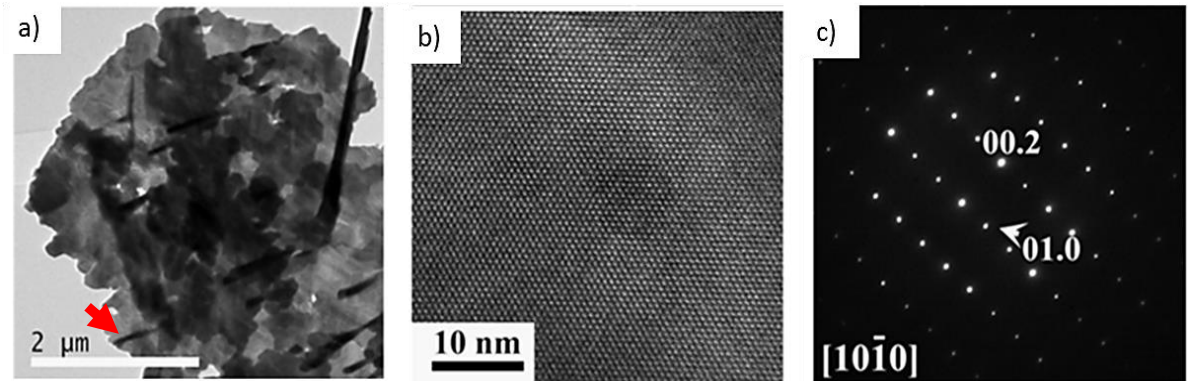

Fig. S4: a) Bright-field TEM image of the hexagonal shape agglomerate, illustrating the nano sized domains constituting the Cu_3P particles; b) HRTEM image; c) corresponding SAED patterns taken along [10$\bar{1}$0] orientation of the domain.

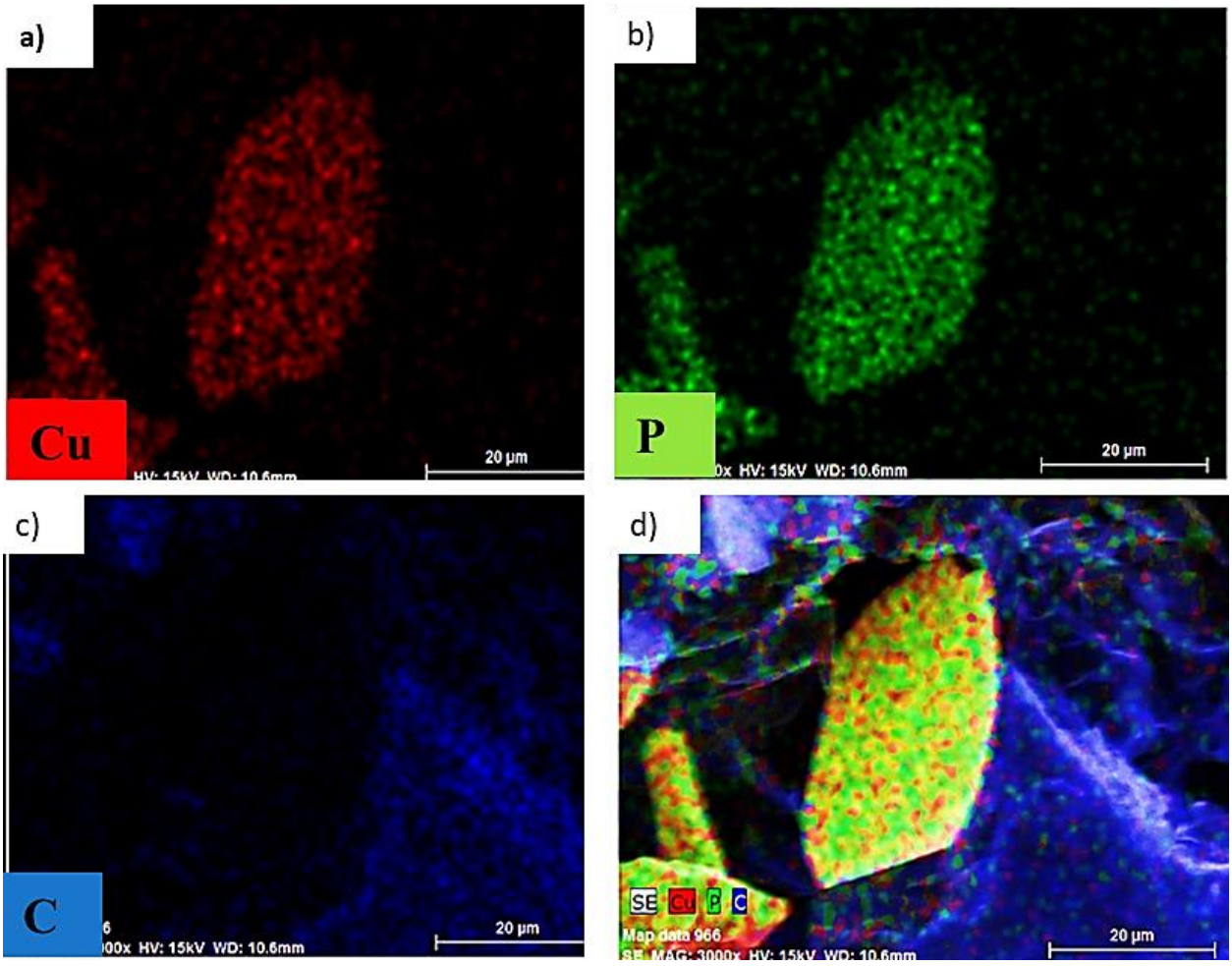

Fig. S5: Cu_3P@3DG the EDS elemental mapping of a) Cu, b) P and c) C elements and d) merge image.

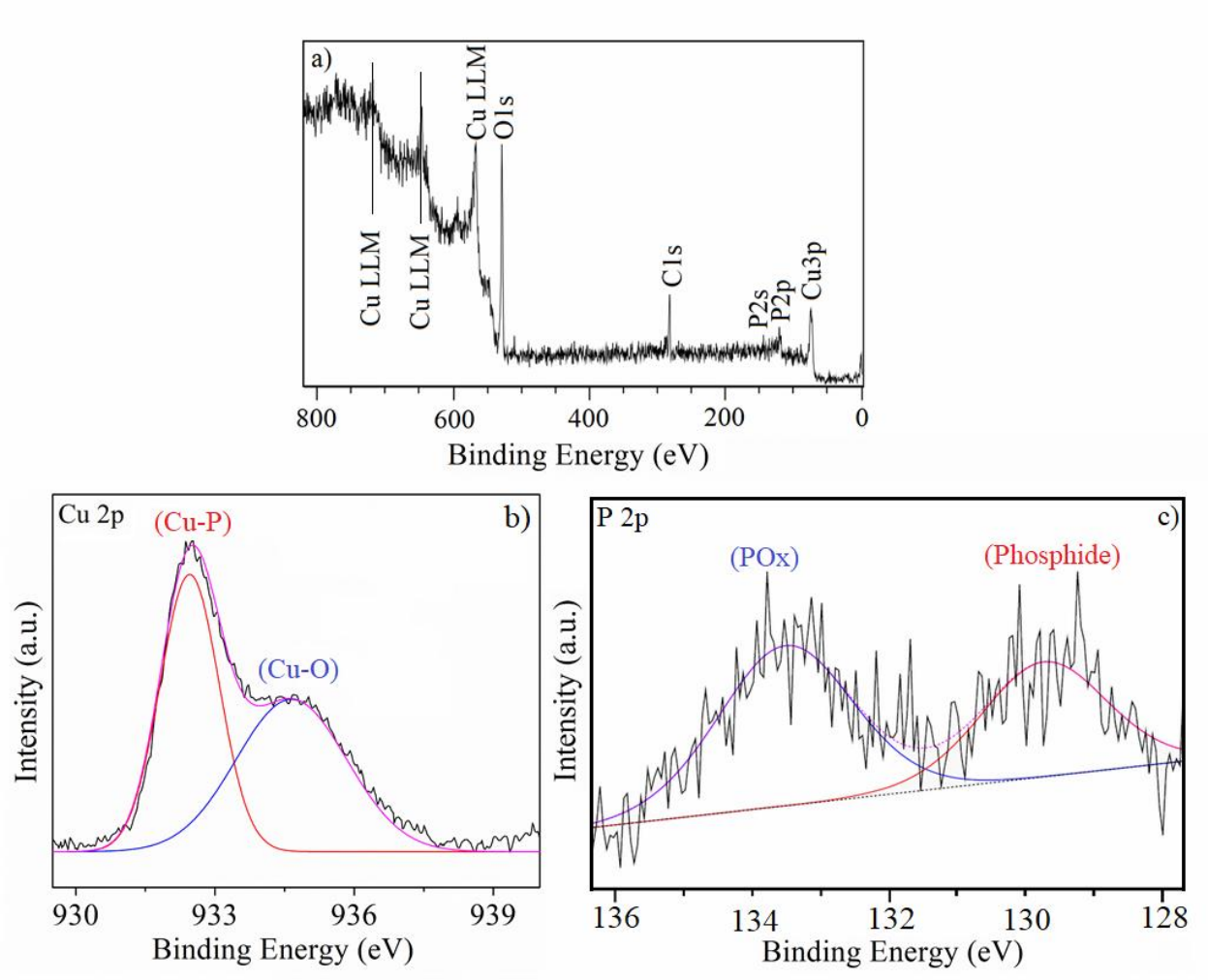

Fig. S6: XPS pattern of Cu_3P: a) survey scan (b- c) high resolution spectra of Cu 2p and P 2p.

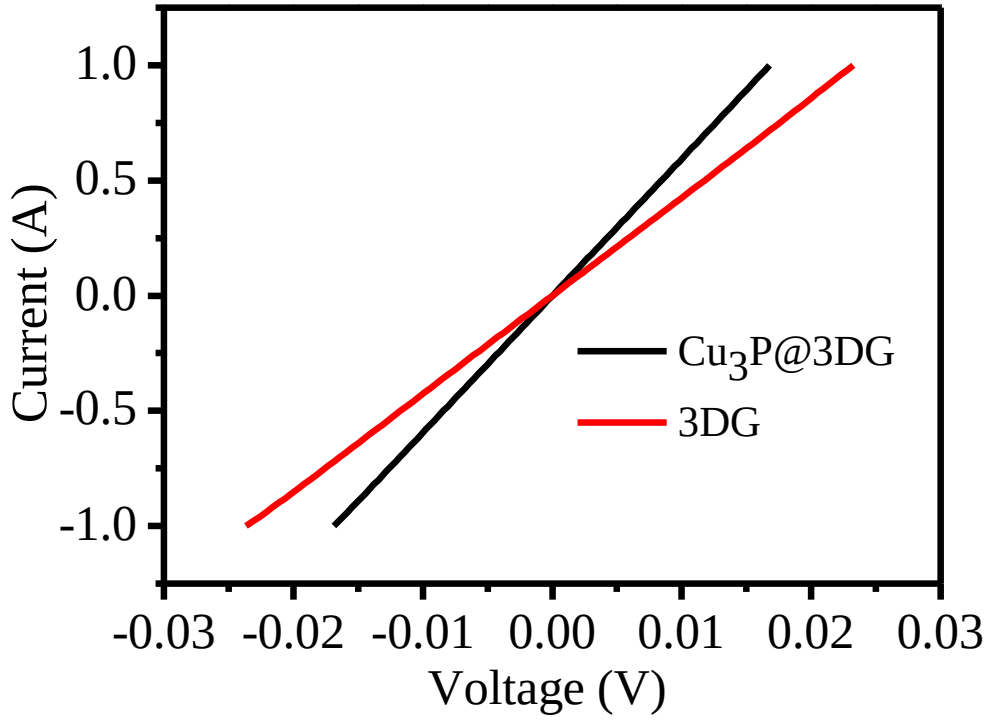

Fig. S7: Conductivity study via 4PP configuration using the source meter unit (Keithley source meter 2450) with 2mm electrode spacing of Cu_3P@3DG and 3DG on graphite substrate where the electrical conductivity was measured to be 1076 S m^{-1} and 978 S m^{-1}respectivily.

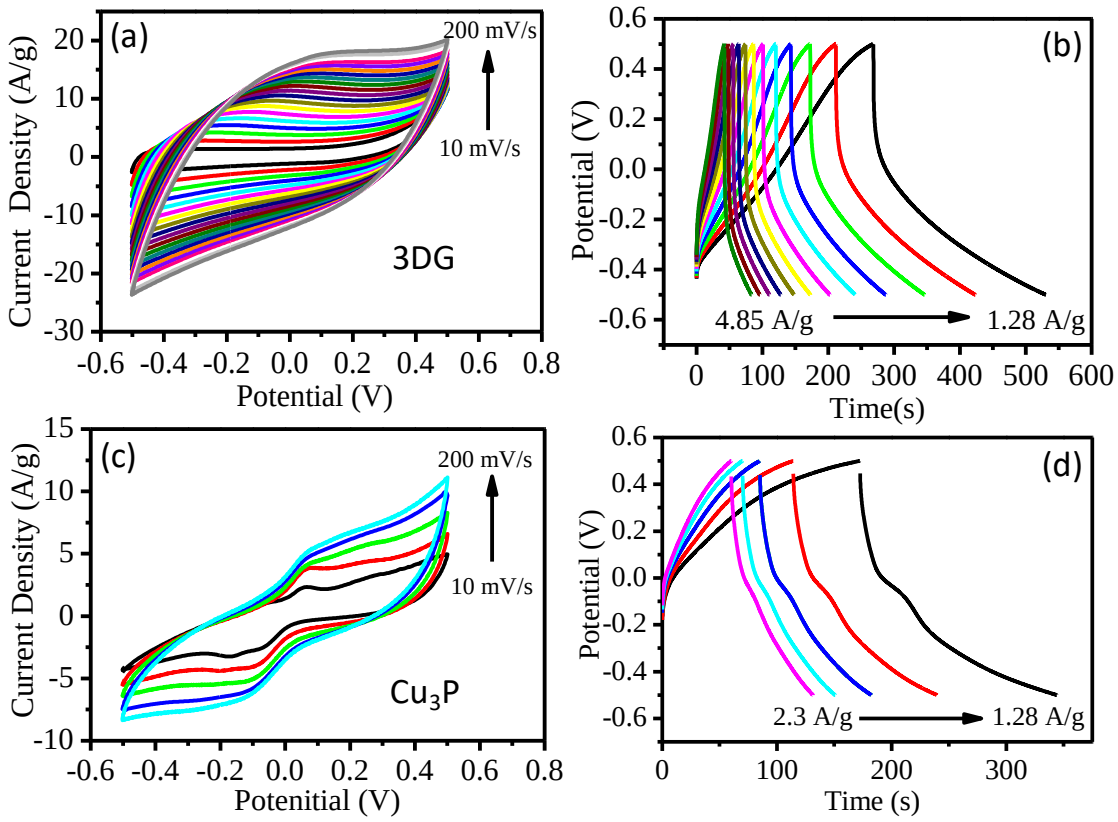

Fig. S8: Electrochemical characterization (a) 3DG CV curves at different scan rate (10 to 200 mV/s); (b) galvanostatic charge-discharge curves obtained at different current densities (1.28, 1.56, 1.85, 2.13, 2.41, 2.69, 2.97, 3.27, 3.7, 4.3, 4.5 and 4.85 A/g); (c) typical CV curves of hexagonal Cu_3P platelets on graphite sheet at different scan rates (10, 50, 100, 150 and 200 mV/s) (b) galvanostatic charge-discharge curves of Cu_3P platelets at various current densities 1.28, 1.67, 1.9, 2.1, and 2.3 A/g).

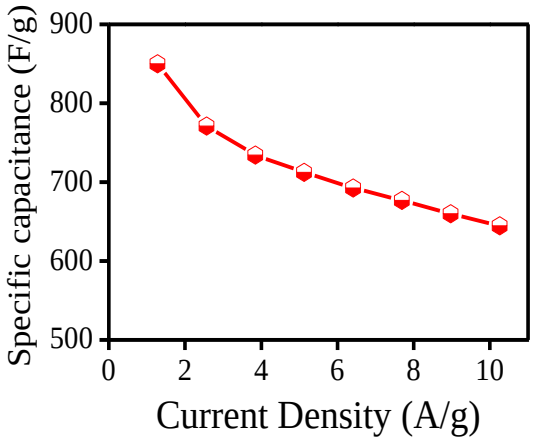

Fig. S9: Variation in gravimetric specific capacitance as a function of the current densities.

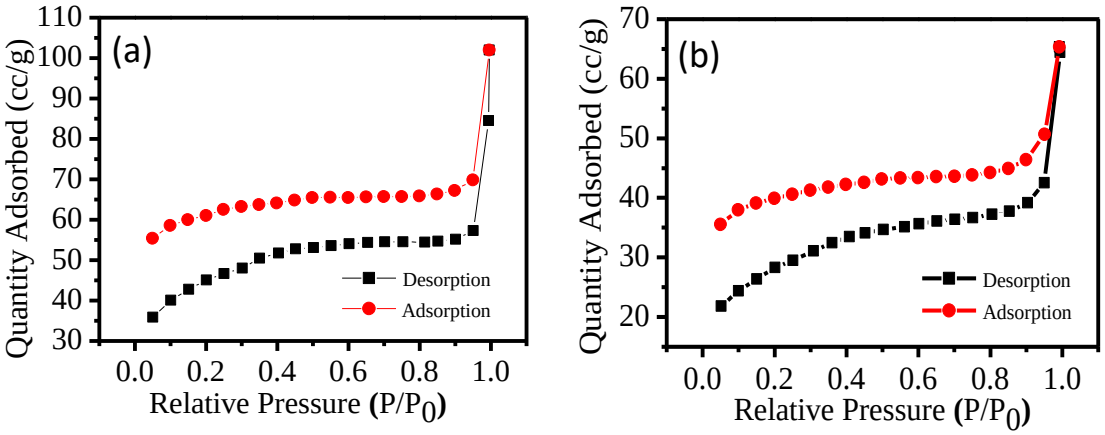

Fig. S10: Nitrogen adsorption-desorption isotherm of the 3DG and the Cu_3P@3DG and corresponding BET specific surface area is 155 and 100 m^2/g.

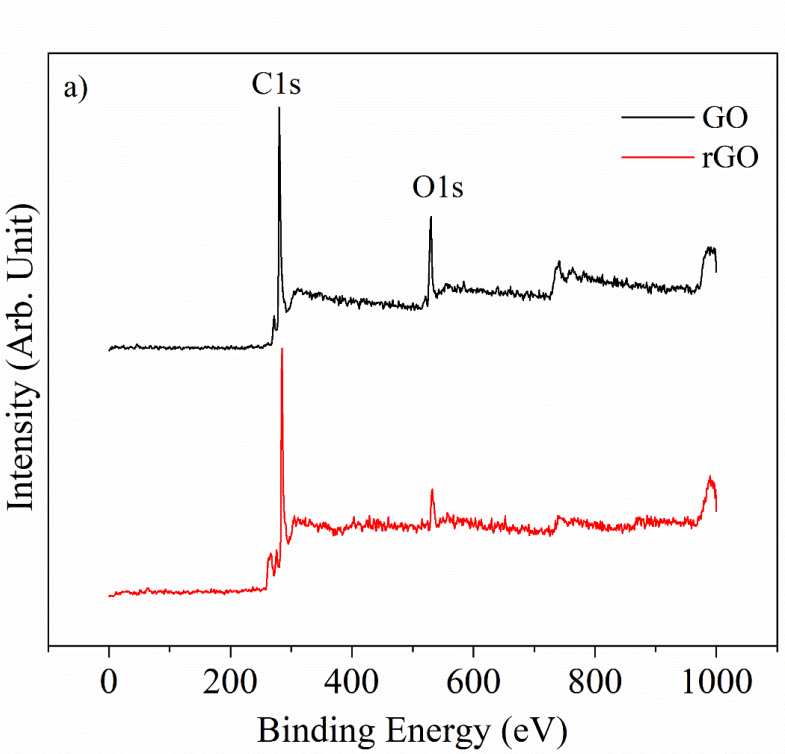

Fig. S11: XPS analysis of GO and rGO samples, where rGO samples are responsible for the formation of 3DG architecture on the solid-state electrode.

The XPS survey scan has been provided for both GO and rGO (responsible for the formation of 3DG matrix) samples. Here it has been observed that while chemical reducing of GO to rGO for the formation of 3DG architecture on a solid-state electrode, there is a significant reduction of O1s peak intensity. This 3DG is acting as a supporting matrix for the formation of nanohybrid with Cu_3P platelets.

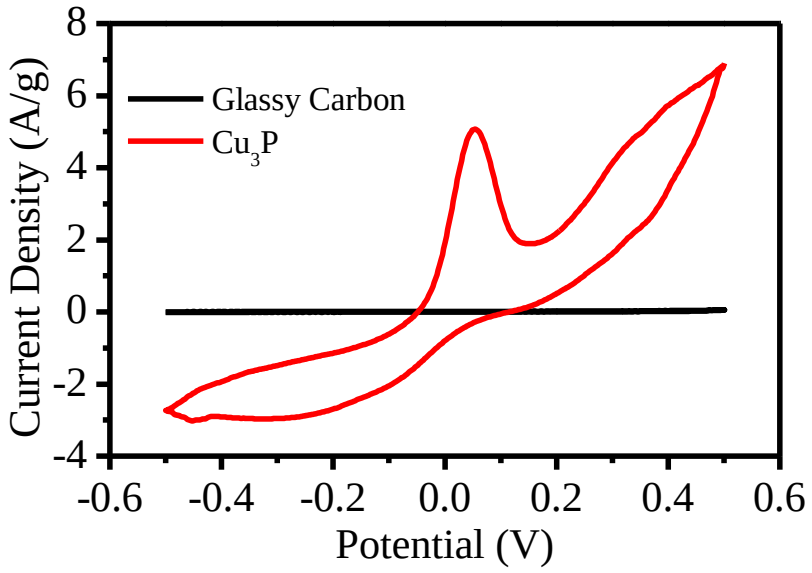

Fig. S12: CV analysis of bare glassy carbon and Cu_3P decorated glassy carbon at 10 mV/s.

References

Jang, G. S., Ameen, S., Akhtar, M. S., Kim, E., and Shin, H. S. (2017). Electrochemical investigations of hydrothermally synthesized porous cobalt oxide (Co3O4) nanorods: supercapacitor application. Chem. Select. 2, 8941–8949. doi: 10.1002/slct.201701571

Jiang, W., Hu, F., Yan, Q., and Wu, X. (2017). Investigation on electrochemical behaviors of NiCo2O4 battery-type supercapacitor electrodes: the role of an aqueous electrolyte. Inorg. Chem. Front. 4, 1642–1648. doi: 10.1039/C7QI00391A

Zeng, L., Lou, X., Zhang, J., Wu, C., Liu, J., and Jia, C. (2019). Carbonaceous mudstone and lignin-derived activated carbon and its application for supercapacitor electrode. Surf. Coatings Technol. 357, 580–586. doi: 10.1016/j.surfcoat.2018.10.041

Zhang, C., Xie, L., Song, W., Wang, J., Sun, G., and Li, K. (2013). Electrochemical performance of asymmetric supercapacitor based on Co3O4/AC materials. J. Electroanaly. Chem. 706, 1–6. doi: 10.1016/j.jelechem. 2013.07.032

Wang, G., Zhang, L., and Zhang, J. (2012b). A review of electrode materials for electrochemical supercapacitors. Chem. Soc. Rev. 41, 797–828. doi: 10.1039/C1CS15060J